Scripta Materialia 259 (2025) 116576

Contents lists available at ScienceDirect

Scripta Materialia

journal homepage: www.journals.elsevier.com/scripta-materialia

Melting temperature, emissivity, and thermal conductivity of rare-earth silicates for thermal and environmental barrier coatings

Hunter B. Schonfeld [a,1], Milena Milich [a,1], Cameron Miller [b], Laura Doumaux [b], Mackenzie Ridley [c], Thomas Pfeifer [a], William Riffe [a], Davide Robba [d], Luka Vlahovic [d], Konstantinos Boboridis [d], Rudy J.M. Konings [d,2], Adam Chamberlain [e], Elizabeth Opila [b], Patrick E. Hopkins [a,b,f,*]

[a] Department of Mechanical and Aerospace Engineering, University of Virginia, 122 Engineer's Way, Charlottesville, VA 22904, USA
[b] Department of Materials Science and Engineering, University of Virginia, 395 McCormick Road, Charlottesville, VA 22904, USA
[c] Oak Ridge National Laboratory, 1 Bethel Valley Road, Oak Ridge, TN 37830, USA
[d] European Commission, Joint Research Centre, Hermann-von-Helmholtz-Straße 1, Eggenstein-Leopoldshafen, 76344, Germany
[e] Rolls-Royce Corporation, 450 S. Meridian Street, Indianapolis, IN 46225, USA
[f] Department of Physics, University of Virginia, 382 McCormick Rd, Charlottesville, VA 22904, USA

ARTICLE INFO

Keywords:
Environmental barrier coatings
Thermal barrier coatings
Thermal conductivity
Solidification
Phase transition

ABSTRACT

In recent years, rare-earth silicates have become the industry standard for coating state-of-the-art SiC ceramic matrix composite (CMC) gas turbine engine components, due to their low volatility, high melting point, and thermal shock resistance. Current research is focused on designing rare-earth silicate based thermal-environmental barrier coatings (T/EBCs) with improved resistance to CMAS (CaO-MgO-Al_2O_3-SiO_2), steam, and crack formation, while maintaining high temperature performance and stability. In this work we compare the high temperature performance of a variety of single and multi-component rare-earth mono- and disilicates (MS, DS) and rare earth apatites by measuring their melting points and spectrally averaged visible emissivities using laser heating and radiation pyrometry. We also report room temperature thermal conductivity measured by time-domain thermoreflectance (TDTR).

In order to achieve greater efficiency, gas turbine engines must be able to operate at higher temperatures. Silicon carbide ceramic matrix composites (CMCs) are promising alternatives to current industry standard nickel superalloys due to their high temperature performance and high strength-to-weight ratio [1]. However, the introduction of SiC in engine components brings about a new set of challenges to overcome. SiC is highly susceptible to steam corrosion [2–5] and reaction with deposits of molten atmospheric debris [6]. A suitable barrier coating for SiC components must therefore not only have a low thermal conductivity and match the coefficient of thermal expansion (CTE) of SiC, but also limit the diffusion of steam and molten debris to the SiC surface. The class of materials collectively referred to as rare earth silicates has emerged as a strong candidate for the next generation of environmental barrier coatings [3,4,7–10].

The materials studied in this work include a variety of rare earth mono- and disilicates and rare earth apatites, as well as several compositionally complex disilicates containing multiple rare earth metals. Compositionally complex materials have received much attention in recent years, especially for high temperature applications, where their high configurational entropy offers the potential for improved stability. Multiple principle component barrier coating materials have been shown to have advantageous thermal and mechanical properties in a number of high temperature applications throughout literature [8,11,12], including low thermal conductivity [8,13] and high hardness and modulus [14–16]. Although rare earth silicates have been well studied up to 1500 °C [8,10,17], the target surface component temperature for CMC combustors and vanes is >1482 °C [18], and few studies have considered these materials at temperatures near melting since the work of Toropov

* Corresponding author.
E-mail address: peh4v@virginia.edu (P.E. Hopkins).
[1] Co-first authors.
[2] Present address: Delft University of Technology, Faculty of Applied Sciences, Department of Radiation Science and Technology, Delft, 2628, Netherlands.

https://doi.org/10.1016/j.scriptamat.2025.116576
Received 19 November 2024; Received in revised form 18 January 2025; Accepted 20 January 2025

Available online 27 January 2025

and Bondar in the 1960s [19–24]. In this work we use a high-power infrared laser to locally heat the silicate samples beyond their melting point and employ a spectrally-resolved radiation pyrometry technique to simultaneously measure melting point and spectrally-averaged visible emittance. We report the resulting melting point and high temperature thermal emittance, hereafter referred to as "emissivity", for a variety of single and multiple principle component rare earth silicates [25,26]. We also measure room temperature thermal conductivity using the optical pump-probe technique, time-domain thermoreflectance [27]. Finally, we investigate the effects of high temperature laser heating and melting on the microstructure of select rare earth silicates through energy dispersive spectroscopy (EDS), and microfocus-Xray diffraction (XRD), reported in *Supplemental Materials*. These measurements are essential to the evaluation of new coating materials that would facilitate increases in gas turbine inlet temperature and improve efficiency in next-generation engines.

Room temperature thermal conductivity was measured via time-domain thermoreflectance (TDTR), as described in *Supplemental Materials*, and the results are plotted in Fig. 1. We find that the single-component disilicates collectively demonstrate substantially higher thermal conductivity than the single-component monosilicates or apatites, with $Sc_2Si_2O_7$ exhibiting a notably high thermal conductivity exceeding 10 $Wm^{-1}K^{-1}$. Although the monosilicates measured have larger rare earth (RE) crystal radii than their disilicate counterparts, this appears to not be the only factor in play. When considering $Yb_2Si_2O_7$ and Yb_2SiO_5, the Yb coordination numbers are very similar, resulting in nearly identical crystal radii. However, the two systems exhibit drastically different thermal conductivities. We hypothesize this is due to greater distortion in the monosilicate lattice [28], leading to increased phonon scattering.

From these results we also observe that the multiple principle component silicates and the rare earth apatite structures exhibited suppressed thermal conductivities, below that predicted by rule of mixtures. The apatites were measured to have particularly low thermal conductivities for this class of materials, approaching the theoretical minimum of their monosilicate counterparts of ~1 $Wm^{-1}K^{-1}$ [4,29]. This is expected due to the presence of cation vacancies in the $RE_{9.33}\square_{0.67}(SiO_4)_6O_2$ structure and large concentrations of oxygen vacancies [30–33] that both act as point defects. This effect has been previously studied in yttrium stabilized zirconia (YSZ). Although Y^{3+} and Zr^{4+} are very similar in size and mass, oxygen vacancies are necessary to preserve the charge balance when zirconia is doped with yttrium to form YSZ [30]. The resulting reduction in conductivity, from ~5 $Wm^{-1}K^{-1}$ in zirconia to ~1.5 $Wm^{-1}K^{-1}$ in YSZ is attributed almost exclusively to phonon scattering at the new oxygen vacancy point defects based on experiments performed on rutile [34]. Similarly in the apatites measured here, these point defects scatter phonons and lead to a significant reduction in thermal conductivity. The low thermal conductivity of apatite, and its potential to limit CMAS infiltration, offers benefits to monosilicate or disilicate EBCs when they are exposed to CMAS and an apatite layer forms on the surface. In the case of the multiple principle component silicate samples, it is instead the high degree of mass disorder between the cations, as well as the resulting distortion in the Si-O tetrahedra that contributes to phonon scattering and the suppressed thermal conductivity observed in these samples, as previously observed by Ridley et al. [8,35], leading to a thermal conductivity below that predicted by rule-of-mixtures.

The low thermal conductivity demonstrated in both the multi-component silicates and the apatite structures is promising for their potential as thermal barrier coatings. Thermal conductivities on the order of YSZ (1.49 $Wm^{-1}K^{-1}$) or lower are necessary to provide a sufficient reduction in temperature between the hot inlet gas temperatures of the engine and the surface of the SiC CMC turbine blade. Low thermal conductivity of apatites along with their high melting temperature recommends them as top candidates for next-generation combined T/EBCs.

The melting temperature of a variety of rare earth silicates and apatite structures was measured by radiation pyrometry, described in detail in *Supplemental Materials*. Briefly, we heat the samples by a high power Nd:YAG laser at 1064 nm. A 256-channel spectropyrometer measures the spectrally resolved radiation intensity from the sample in the 500-1000 nm wavelength range while a single-wavelength pyrometer operating at 663 nm measures surface radiance temperature with a higher temporal resolution. A set of example thermograms is shown in Fig. 2. We measure the melting temperature as the temperature of the thermal arrest associated with resolidification upon cooling. Trials of each sample were conducted in both 1.5 bar argon and ambient air environments. Although many of the samples were observed to change color when heated in argon, when we compare the measured melting temperature between the two environments, we find that with the exception of Gd_2SiO_5 and LaGd apatite, the presence of an inert atmosphere does not impact the melting point of the silicate samples, and we therefore average the results of trials in air and argon to calculate the reported melting temperature. We hypothesize that the darkening of the samples at high temperatures in argon is due to the creation of oxygen vacancies in the high temperature, low-oxygen environment, as this is also observed in silicates sintered via spark plasma sintering (SPS) in argon. Material darkening due to oxygen vacancies can occur at very low vacancy concentrations, affecting the optical properties while not affecting the material's mechanical properties. This results in much higher absorption at the laser wavelength, allowing us to reach melting temperatures with much less laser power. The sample subsequently returns to its original color when it is heated in air. In the case of Gd_2SiO_5 and LaGd apatite, we not only observe a color change when the samples are heated in argon, but an increase in emissivity and a ~100 K decrease in melting temperature. We report the results of the trials conducted in argon for these samples, as they more closely resemble the conditions of Toropov and Bondar's experiments on the Gd_2O_3-SiO_2 system, which were conducted under vacuum [20]. The results of all melting point experiments are shown in Fig. 3.

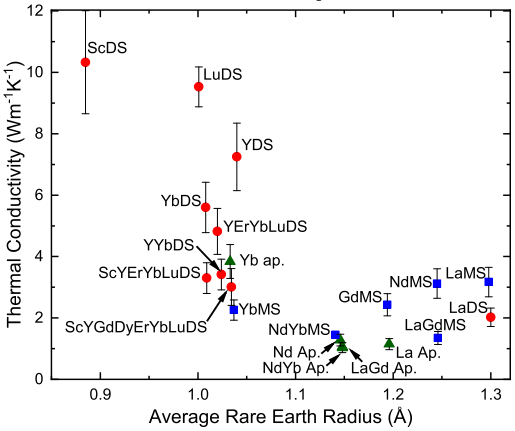

Fig. 1. Thermal conductivity at 300 K is measured by time-domain thermoreflectance (TDTR) and plotted as a function of rare earth cation radius.

We observe that for silicates of the same rare earth element, the monosilicate has a higher melting point than the disilicate, as evidenced by the La and Yb silicates. This is in agreement with the trends present in phase diagrams developed by Toropov and Bondar [21,19], and as also calculated by Ye, et al. [37]. In general, the apatite samples demonstrated even higher melting points than their monosilicate counterparts, with Yb apatite being the exception. Yb apatite however, exhibited a second thermal arrest at 2203 K. Further characterization of the sample via XRD revealed that the Yb_2SiO_5 and $Yb_2Si_2O_7$ constituent powders remained unreacted in the sintered Yb apatite sample, and remained a two-phase system. We thus observed the melting points of the disilicate and monosilicate phases through two distinct resolidifications. The two-, four- and five-component rare earth disilicates are observed to have high melting temperatures, competitive with their single-component counterparts and undiminished by their compositional disorder. This is encour-

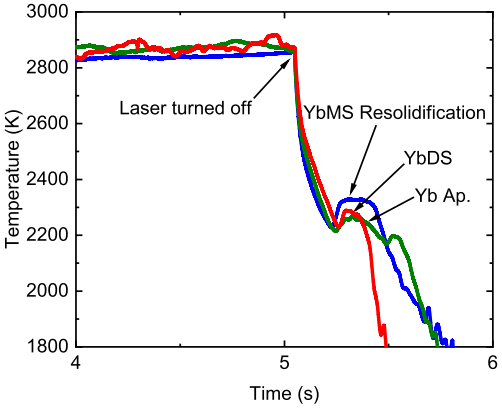

Fig. 2. Thermograms of Yb_2SiO_5, $Yb_2Si_2O_7$, and Yb apatite cooling from melt, with the solidification plateau indicated.

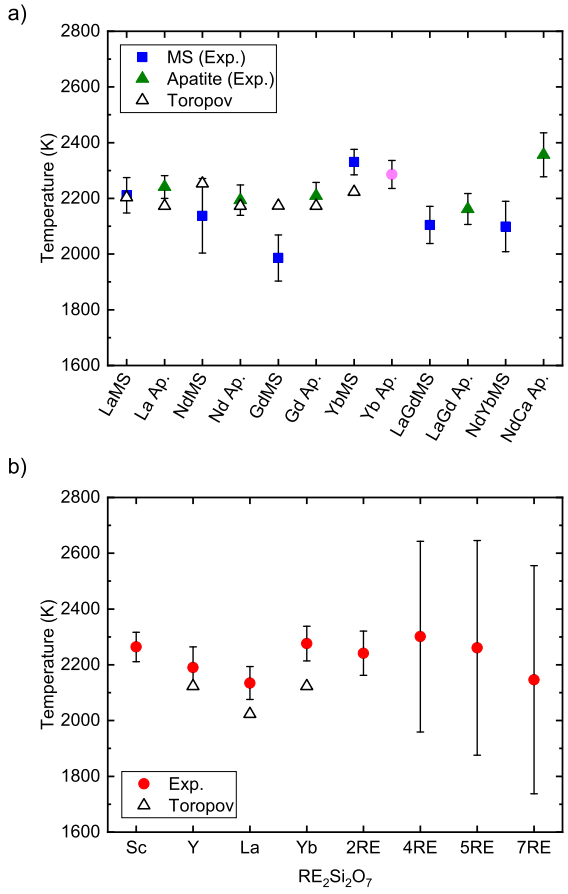

Fig. 3. Experimentally determined melting point for a) RE monosilicates and apatites and b) RE disilicates, compared against previous measurements by Toropov and Bondar [19–22,36,24]. Note: Yb ap. sample is unreacted two-phase mixture of Yb_2SiO_5 and $Yb_2Si_2O_7$.

aging as it demonstrates the possibility of tuning high-temperature thermal and mechanical properties through selection of rare earth cations without compromising melting temperature.

Previous studies on the melting point of rare earth oxides (RE_2O_3) [38–41] have found linear trends with the rare earth ionic radius, as well as the number of electrons in the $4f$ orbital of the RE. For these oxides, the melting point decreases with increasing ionic radius, and increases with increasing number of electrons in the rare earth's $4f$ orbital. This is to be expected as the distance between the atoms is indicative of the bond strength. With this reasoning in mind, we similarly expect the melting point of rare earth mono- and disilicates to trend with rare earth radius. It has been shown previously in $X1$ type monosilicates and apatite structures that elastic modulus increases with decreasing rare earth ionic radius [42,43]. As the bond length of the [SiO_4] tetrahedra is less impacted by changes in RE cation than the bonding in the REO_x polyhedra [44], we anticipate trends previously observed in RE oxides to be representative of the RE silicates as well. However, the results of our melting temperature measurement do not trend with rare earth radius or calculated elastic modulus. If we instead look to the average interatomic force constants, as calculated for a variety of $RE_2Si_2O_7$ polymorphs by Luo et al. [45], we see that interatomic force trends only weakly with RE ion, and is far more dominated by phase than RE ion. Additionally, Luo et al. observe that the average interatomic force constants for the Si-O bonds are more than five times greater than those of the RE-O bonds. Considering the weak trend in RE-O bond strength with RE ion and the relative weakness of the RE-O bond in general, it is reasonable that we observe little change in melting temperature with RE crystal radius.

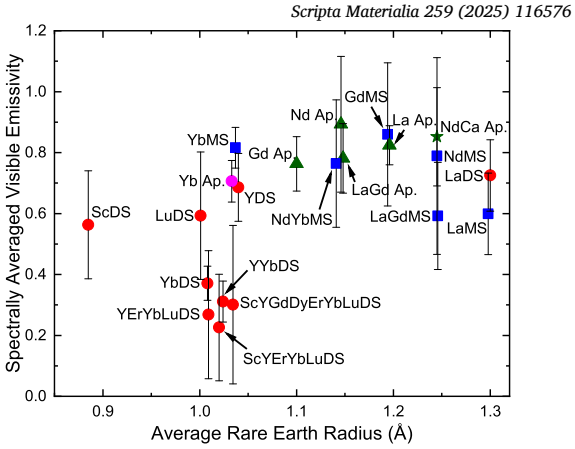

Fig. 4. Spectrally averaged visible emissivity at the materials' respective melting temperature plotted as a function of rare earth cation radius. Red circles represent RE disilicate samples, blue squares designate monosilicates, and green triangles designate apatites. (For interpretation of the colors in the figure(s), the reader is referred to the web version of this article.)

To investigate the effects of compositional disorder on melting point, a number of multi-component silicate systems were measured as well. The four and five-component disilicates had the highest melting temperatures recorded for the multi-component disilicate samples with values of 2301±249 K and 2261±351 K, exceeding that of the seven-component system. The large uncertainty associated with the experiments on the compositionally complex materials is due to both low emissivity and the large number of intertwining spectral features, similar to those seen in oxides of erbium [46], that are still present at these temperatures resulting in higher uncertainty in the linear fit of radiance temperatures. Despite the large uncertainties reported with these values, we are confident that the compositionally complex disilicates offer a new avenue to low thermal conductivity EBC with competitive melting temperatures.

The spectral intensity of radiation from each sample is measured at its respective resolidification point as detailed in *Supporting Information*. This distribution is analyzed using the described linear approximation of inverse temperatures to calculate the spectrally-averaged normal emissivity from 550-700 nm of the samples near the solid-liquid phase transition, as identified by the thermal arrest during resolidification. The measured emissivities are reported in Fig. 4. We note that although we refer to these values by the term "emissivity", this measurement is subject to both the properties of the samples as prepared, and the dynamic nature of the resolidification experiment itself, and thus are not a measurement of the intrinsic emissivity of the RE_2SiO_5 and $RE_2Si_2O_7$ systems. However, the measured thermal emittance at resolidification

is interesting in its own right and it is worth discussing the observed trends.

It was unexpected that the monosilicates and apatites displayed such high emissivities regardless of RE ion. Previous studies on the optical properties of RE zirconates have demonstrated manipulation of absorption in the near-IR through RE dopant selection [47], including enhancement of optical properties across the visible and near-IR spectra through multiple-cation contributions. However, these experiments were conducted at room temperature. In our high-temperature measurements, we observe a systematic increase of emissivity in RE monosilicates and apatites, as well as some disilicates. We hypothesize that the high emissivity observed in the RE apatites and monosilicates is due to increased vacancy concentration in addition to the expected broadening associated with high temperatures. The effect of oxygen vacancies and point defects has been studied previously in silica, zirconia, and samaria by Avdoshenko and Strachan [48]. It was determined through DFT calculations that oxygen vacancies led to a substantial increase in emissivity at 2000 K in both zirconia and samaria. This hypothesis is further supported by our observations on the Gd_2SiO_5 system, which exhibited a considerably higher emissivity when melted in argon than when melted in air, likely due to an increase in oxygen vacancies that formed when the sample was heated in the absence of oxygen.

The emissivity of these coating materials at high temperature is critical to their potential as a combined thermal and environmental barrier coating. Low emissivity implies not only limited radiative heat dissipation, but direct radiative heating of the underlying bond coat or component from the hot combustion gases in the engine. By increasing the emissivity, and thus absorption, of the coating material in the visible and near-IR regime, the temperature at the coating/component interface can be dramatically reduced, allowing for higher engine operating temperatures [47,49]. Based on the experimental results of the present study, RE monosilicates and apatites may be more favorable as radiative barrier coatings at high temperatures. Further experimentation is needed to determine the mechanisms of the observed dramatic enhancement of emissivity at high temperature, and our future work aims to characterize the temperature dependence of emissivity in these RE silicate systems.

In summary, we have determined the melting temperature, normal spectrally averaged visible emissivities, and thermal conductivities of a number of rare earth silicate and apatite compounds. These thermal properties are critical to evaluating materials' suitability for the high temperature conditions of a gas turbine engine. Although it is difficult to recommend a specific silicate composition based on thermal conductivity, emissivity, and melting temperature alone, based on these results, we can, however, rule out materials with especially low melting points, such as Gd_2SiO_5, or silicates containing lanthanum, which exhibited signs of silica volatilization, as potential candidates for a next-generation EBC. By studying such a variety of silicate systems, we can better predict the effects of RE cation, compositional complexity and crystal structure on high temperature behavior and guide the design of the next generation of thermal and environmental barrier coatings.

CRediT authorship contribution statement

Hunter B. Schonfeld: Writing – original draft, Investigation, Formal analysis. **Milena Milich:** Writing – original draft, Visualization, Methodology, Investigation, Formal analysis. **Cameron Miller:** Resources, Investigation. **Laura Doumaux:** Resources, Investigation. **Mackenzie Ridley:** Writing – review & editing, Resources. **Thomas Pfeifer:** Investigation. **William Riffe:** Investigation. **Davide Robba:** Writing – review & editing, Resources, Methodology. **Luka Vlahovic:** Writing – review & editing, Resources, Methodology. **Konstantinos Boboridis:** Writing – review & editing, Resources, Methodology. **Rudy J.M. Konings:** Supervision, Resources. **Adam Chamberlain:** Supervision, Project administration, Funding acquisition, Conceptualization. **Elizabeth Opila:** Supervision, Resources, Project administration, Funding acquisition, Conceptualization. **Patrick E. Hopkins:** Writing – review & editing, Supervision, Resources, Project administration, Methodology, Funding acquisition, Conceptualization.

Declaration of competing interest

The authors declare that they have no known competing financial interests or personal relationships that could have appeared to influence the work reported in this paper.

Acknowledgements

We appreciate support from the Office of Naval Research, Grant Number N00014-21-1-2477 and Rolls-Royce, Project Number 25-UVA-26. We are also grateful to Dr. Prasanna Balachandran and Ryan Grimes of the University of Virginia for their collaboration and insight regarding the emissivity of rare earth silicates.

Appendix. Supplementary material

Supplementary material related to this article can be found online at https://doi.org/10.1016/j.scriptamat.2025.116576.

References

[1] N.P. Padture, Advanced structural ceramics in aerospace propulsion, Nat. Mater. 15 (2016) 804–809, https://doi.org/10.1038/nmat4687.

[2] D. Tejero-Martin, M. Bai, A.R. Romero, R.G. Wellman, T. Hussain, Steam degradation of ytterbium disilicate environmental barrier coatings: effect of composition, microstructure and temperature, J. Therm. Spray Technol. 32 (2023) 29–45.

[3] D.H. Olson, J.A. Deijkers, K. Quiambao-Tomko, J.T. Gaskins, B.T. Richards, E.J. Opila, P.E. Hopkins, H.N.G. Wadley, Evolution of microstructure and thermal conductivity of multifunctional environmental barrier coating systems, Mater. Today Phys. 17 (2021).

[4] L.R. Turcer, N.P. Padture, Towards multifunctional thermal environmental barrier coatings (tebcs) based on rare-earth pyrosilicate solid-solution ceramics, Scr. Mater. 154 (2018) 111–117.

[5] D. Tejero-Martin, C. Bennett, T. Hussain, A review on environmental barrier coatings: history, current state of the art and future developments, J. Eur. Ceram. Soc. 41 (2021) 1747–1768, https://doi.org/10.1016/j.jeurceramsoc.2020.10.057.

[6] J. Liu, L. Zhang, Q. Liu, L. Cheng, Y. Wang, Calcium–magnesium–aluminosilicate corrosion behaviors of rare-earth disilicates at 1400°c, J. Eur. Ceram. Soc. 33 (2013) 3419–3428.

[7] M. Ridley, K. Kane, M. Lance, C. Parker, Y.F. Su, S. Sampath, E. Garcia, M. Sweet, M. O'Connor, B. Pint, Steam oxidation and microstructural evolution of rare earth silicate environmental barrier coatings, J. Am. Ceram. Soc. 106 (2023) 613–620.

[8] M. Ridley, J. Gaskins, P. Hopkins, E. Opila, Tailoring thermal properties of multi-component rare earth monosilicates, Acta Mater. 195 (2020) 698–707.

[9] B.T. Richards, K.A. Young, F. de Francqueville, S. Sehr, M.R. Begley, H.N. Wadley, Response of ytterbium disilicate-silicon environmental barrier coatings to thermal cycling in water vapor, Acta Mater. 106 (2016) 1–14.

[10] N.A. Nasiri, N. Patra, D. Horlait, D.D. Jayaseelan, W.E. Lee, Thermal properties of rare-earth monosilicates for EBC on Si-based ceramic composites, J. Am. Ceram. Soc. 99 (2016) 589–596.

[11] S. Akrami, P. Edalati, M. Fuji, K. Edalati, High-entropy ceramics: review of principles, production and applications, Mater. Sci. Eng., R Rep. 146 (2021) 100644.

[12] Y. Luo, L. Sun, J. Wang, T. Du, C. Zhou, J. Zhang, J. Wang, Phase formation capability and compositional design of β -phase multiple rare-earth principal component disilicates, Nat. Commun. 14 (2023) 1275.

[13] J.L. Braun, C.M. Rost, M. Lim, A. Giri, D.H. Olson, G.N. Kotsonis, G. Stan, D.W. Brenner, J.-P. Maria, P.E. Hopkins, Charge-induced disorder controls the thermal conductivity of entropy-stabilized oxides, Adv. Mater. 30 (2018) 1805004.

[14] Y.J. Zhou, Y. Zhang, Y.L. Wang, G.L. Chen, Solid solution alloys of alcocrfeni tix with excellent room-temperature mechanical properties, Appl. Phys. Lett. 90 (2007) 181904.

[15] Y. Wang, T. Csanádi, H. Zhang, J. Dusza, M.J. Reece, R.Z. Zhang, Enhanced hardness in high-entropy carbides through atomic randomness, Adv. Theory Simul. 3 (2020) 2000111.

[16] D.G. Sangiovanni, W. Mellor, T. Harrington, K. Kaufmann, K. Vecchio, Enhancing plasticity in high-entropy refractory ceramics via tailoring valence electron concentration, Mater. Des. 209 (2021) 109932.

[17] Z. Tian, L. Zheng, Z. Li, J. Li, J. Wang, Exploration of the low thermal conductivities of γ-y2si2o7, β-y2si2o7, β-yb2si2o7, and β-lu2si2o7 as novel environmental barrier coating candidates, J. Eur. Ceram. Soc. 36 (2016) 2813–2823, https://doi.org/10.1016/j.jeurceramsoc.2016.04.022.

[18] M. Halbig, M. Jaskowiak, J. Kiser, D. Zhu, Evaluation of ceramic matrix composite technology for aircraft turbine engine applications, in: 51st AIAA Aerospace Sciences Meeting Including the New Horizons Forum and Aerospace Exposition, American Institute of Aeronautics and Astronautics, 2013.

[19] N.A. Toropov, I.A. Bondar, Silicates of rare-earth elements - communication 4. New silicates in the system la2o3-sio3, Bull. Acad. Sci. USSR Div. Chem. Sci. 10 (1961) 682–687.

[20] N.A. Toropov, F.Y. Galakhov, S.F. Konovalova, Silicates of the rare earth elements - communication 2. Phase diagram of the binary system gadolinium oxide-silica, Bull. Acad. Sci. USSR Div. Chem. Sci. 10 (1961) 497–501.

[21] N.A. Toropov, I.A. Bondar, Silicates of the rare earth elements - communication 3. Phase diagram of the binary system yttrium oxide-silica, Bull. Acad. Sci. USSR Div. Chem. Sci. 10 (1961) 502–508.

[22] N.A. Toropov, I.A. Bondar, Silicates of the rare earth elements - communication 6. Phase diagrams of the binary systems sm2o3-sio2 and yb2o3-sic2, and comparison of these silicates with the other rare earth element silicates which have been studied, Bull. Acad. Sci. USSR Div. Chem. Sci. 10 (1961) 1278–1285.

[23] N.A. Toropov, V.A. Vasil'Eva, Equilibrium diagram of the scandium oxide-silica binary system, Russian J. Inorg. Chem. 7 (1962) 1001.

[24] I.A. Bondar, N.A. Toropov, Preparation and properties of rare-earth silicates and aluminates, Mater. Res. Bull. 2 (1967) 479–489.

[25] D. Manara, C. Ronchi, M. Sheindlin, M. Lewis, M. Brykin, Melting of stoichiometric and hyperstoichiometric uranium dioxide, J. Nucl. Mater. 342 (2005) 148–163.

[26] D. Manara, M. Sheindlin, W. Heinz, C. Ronchi, M. Sheindlin, W. Heinz, C. Ronchi, New techniques for high-temperature melting measurements in volatile refractory materials via laser surface heating, Rev. Sci. Instrum. 79 (2008) 11.

[27] C.A. Paddock, G.L. Eesley, Transient thermoreflectance from thin metal films, J. Appl. Phys. 60 (1986) 285–290.

[28] H. Xiang, Z. Feng, Y. Zhou, Mechanical and thermal properties of yb 2 sio 5: first-principles calculations and chemical bond theory investigations, J. Mater. Res. 29 (2014) 1609–1619, https://doi.org/10.1557/jmr.2014.201.

[29] Z. Tian, L. Zheng, J. Wang, P. Wan, J. Li, J. Wang, Theoretical and experimental determination of the major thermo-mechanical properties of re2sio5 (re = tb, dy, ho, er, tm, yb, lu, and y) for environmental and thermal barrier coating applications, J. Eur. Ceram. Soc. 36 (2016) 189–202.

[30] Z. Qu, T.D. Sparks, W. Pan, D.R. Clarke, Thermal conductivity of the gadolinium calcium silicate apatites: effect of different point defect types, Acta Mater. 59 (2011) 3841–3850.

[31] T. Allen, J. Graser, R. Issa, T.D. Sparks, Thermoelectric properties of TaVO5 and GdTaO4: an experimental verification of machine learning prediction, Adv. Appl. Ceram., Struct. Funct. Bioceram. 1 (2024), https://doi.org/10.1177/17436753231213060.

[32] H. Zhang, J. Lu, X. Shan, D. Wu, X. Zhao, F. Guo, P. Xiao, A promising molten silicate resistant material: rare-earth oxy-apatite re9.33(sio4)6o2 (re = gd, nd or la), J. Eur. Ceram. Soc. 40 (2020) 4101–4110, https://doi.org/10.1016/j.jeurceramsoc.2020.04.021.

[33] M.R. Winter, D.R. Clarke, Oxide materials with low thermal conductivity, J. Am. Ceram. Soc. 90 (2007) 533–540, https://doi.org/10.1111/j.1551-2916.2006.01410.x.

[34] P.G. Klemens, Phonon scattering by oxygen vacancies in ceramics, Physica B, Condens. Matter 263–264 (1999) 102–104.

[35] X. Liu, P. Zhang, M. Huang, Y. Han, N. Xu, Y. Li, Z. Zhang, W. Pan, C. Wan, Effect of lattice distortion in high-entropy re2si2o7 and re2sio5 (re = ho, er, y, yb, and sc) on their thermal conductivity: experimental and molecular dynamic simulation study, J. Eur. Ceram. Soc. 43 (2023) 6407–6415, https://doi.org/10.1016/J.JEURCERAMSOC.2023.06.052.

[36] N.A. Toropov, F.Y. Galakhov, S.F. Konovalova, Silicates of the rare earths, Bull. Acad. Sci. USSR Div. Chem. Sci. 11 (1962) 689–693, https://doi.org/10.1007/BF00905284.

[37] X. Ye, Y. Luo, S. Liu, D. Wu, D. Hou, F. Yang, Experimental study and thermodynamic calculation of lu 2 o 3 -sio 2 binary system, J. Rare Earths 35 (2017) 927–933.

[38] M. Pianassola, K.L. Anderson, J. Safin, C. Agca, J.W. McMurray, B.C. Chakoumakos, J.C. Neuefeind, C.L. Melcher, M. Zhuravleva, Tuning the melting point and phase stability of rare-earth oxides to facilitate their crystal growth from the melt, J. Adv. Ceram. 11 (2022) 1479–1490, https://doi.org/10.1007/s40145-022-0625-z.

[39] J. Hlavac, Melting temperatures of refractory oxides: Part i, Pure Appl. Chem. 54 (1982) 681–688, https://doi.org/10.1351/pac198254030681.

[40] J.P. Coutures, M.H. Rand, Melting temperatures of refractory oxides - part ii: lanthanoid sesquioxides, Pure Appl. Chem. 61 (1989) 1461–1482, https://doi.org/10.1351/pac198961081461.

[41] A. Navrotsky, W. Lee, A. Mielewczyk-Gryn, S.V. Ushakov, A. Anderko, H. Wu, R.E. Riman, Thermodynamics of solid phases containing rare earth oxides, J. Chem. Thermodyn. 88 (2015) 126–141, https://doi.org/10.1016/J.JCT.2015.04.008.

[42] Z. Tian, J. Zhang, T. Zhang, X. Ren, W. Hu, L. Zheng, J. Wang, Towards thermal barrier coating application for rare earth silicates re2sio5 (re = la, nd, sm, eu, and gd), J. Eur. Ceram. Soc. 39 (2019) 1463–1476, https://doi.org/10.1016/j.jeurceramsoc.2018.12.015.

[43] R. Wu, W. Pan, X. Ren, C. Wan, Z. Qu, A. Du, An extremely low thermal conduction ceramic: Re9.33(sio4)6o2 silicate oxyapatite, Acta Mater. 60 (2012) 5536–5544, https://doi.org/10.1016/j.actamat.2012.06.051.

[44] Q. Wang, J. Huang, A DFT-based descriptor to predict the water vapor corrosion resistance of rare-earth monosilicates, Materials 15 (2022) 2414, https://doi.org/10.3390/ma15072414.

[45] Y. Luo, L. Sun, J. Wang, Z. Wu, X. Lv, J. Wang, Material-genome perspective towards tunable thermal expansion of rare-earth di-silicates, J. Eur. Ceram. Soc. 38 (2018) 3547–3554, https://doi.org/10.1016/j.jeurceramsoc.2018.04.021.

[46] G.E. Guazzoni, High-temperature spectral emittance of oxides of erbium, samarium, neodymium and ytterbium, Appl. Spectrosc. 26 (1972) 60–65, https://doi.org/10.1366/000370272774352597.

[47] Q. Flamant, D.R. Clarke, Opportunities for minimizing radiative heat transfer in future thermal and environmental barrier coatings, Scr. Mater. 173 (2019) 26–31, https://doi.org/10.1016/j.scriptamat.2019.07.041.

[48] S.M. Avdoshenko, A. Strachan, High-temperature emissivity of silica, zirconia and samaria from ab initio simulations: role of defects and disorder, Model. Simul. Mater. Sci. Eng. 22 (2014) 075004, https://doi.org/10.1088/0965-0393/22/7/075004.

[49] V.K. Champagne, G. Pisaturo, D.R. Clarke, High temperature oxides for selective absorption of thermal radiation, J. Eur. Ceram. Soc. 43 (2023) 7656–7667, https://doi.org/10.1016/J.JEURCERAMSOC.2023.07.075.